

Autonomous Bird Deterrent System for Vineyards using Multiple Bio-inspired Unmanned Aerial Vehicle

Z. Wang*, and KC Wong
University of Sydney, Australia

ABSTRACT

A novel bird deterrent system using multiple Unmanned Aerial Vehicles (UAVs) for vineyards is being proposed. Bird damage in agriculture is a significant and long-standing problem globally. A successful bird deterring system must be effective and autonomous to eliminate cost associated with human operator. In this paper, we derive the hardware requirement for such a system from experimental data, as well as a bird deterring strategy to enable autonomous operation. The hardware and strategy are first tested under manual control to assess effectiveness. The problem of trajectory planning for UAVs is formulated as a model predictive control problem. Models of the bird detection sensor, the bird behaviour, the UAV dynamics and the environment are estimated using experimental data. Occupancy grid map is used to represent the state of the environment, and this map is used to plan the optimal bird deterring trajectory for UAVs. Preliminary results from the simulation indicated that a 40-hectare vineyard can be protected by two UAVs.

1 INTRODUCTION

Managing pest bird damage in agriculture is a challenging problem because of the scale of agriculture sites and unpredictability of wildlife. In Australia, around AU\$300 million worth of commercial crops are lost due to pest bird damage [1]; the estimates in the United States may well exceed US\$4.7 billion [2]. Many methods have been developed, yet there are only a few effective but expensive methods [3]. Wine grape is one of the most vulnerable commercial crops to bird damage. Netting is the most common methods deployed in vineyards. However, the cost of netting increases as the size of the vineyard increases, making this method too expensive for large vineyards.

With the fast development of UAV and autonomous technologies, there are increasingly more interests in using UAVs for bird damage control among researchers and grape growers. UAVs have the advantage of traversing a large agriculture property in a relatively short period of time compared to ground vehicles. They are also not constrained by rough terrains commonly found in agriculture properties.

*Email address: zwan7346@uni.sydney.edu.au



Figure 1: A photo of the prototype UAV.

The aim of this research is to develop a autonomous UAV bird deterring system for agriculture. The problem in vineyards will be investigated first. There are many challenges to be addressed, including finding the most effective scaring elements; determining the appropriate sensors for bird detection; the ground-to-air communication; and developing the deterring strategy. Such a system will also be desirable in other situations where bird populations may cause damage or are nuisance. These examples include but not limited to: airport, chemical spill sites, aircraft hangars, trains stations and private spaces.

2 RELATED WORK

Natural predatory birds are most efficient at deterring pest birds. A trial conducted on a New Zealand vineyard saw the grape damage reduce by 95% after introducing the New Zealand Falcon in the region [4]. However, hoping for an eagle to appear every time the pest birds are coming is unrealistic. Many commercial solutions and published researches that utilise UAVs to mimic predators exploit neophobia (fear of novel objects) in the pest birds [5]. These UAV methods are indifferent to conventional scaring methods (e.g. scare crows, loud and sudden noises from speakers) as they may also suffer from habituation. Habituation is where the pest birds learn that the UAVs are not real threat and stop associating the UAVs with danger. To avoid habituation, we need to understand the triggers for a long term anti-predatory behaviour. The most important lesson learned from literature is that birds obtain information about predation risk from each

other [6]. Birds typically produce anti-predator vocalisations (also known as alarm and distress calls) when a natural predator is spotted. Birds can learn about new predators if a real threat is accompanying the calls [7]. This is the approach implemented in the prototype system.

An autonomous system must also know where the birds are. Bird detection has always been a challenging problem. The birds are not only naturally camouflaged, they are always morphing during flight as well. The problem can be however simplified in this application as the exact number of birds is not important for the decision process, only pest birds that move in large flock are of concern to the vineyard growers.

An appropriate trajectory planning algorithm is also required for autonomous operation. There are many uncertain variables in the environment, such as the bird location and the bird behaviour. Occupancy grid mapping is one of the most appropriate algorithm for this system, it is commonly implemented in 2D autonomous vehicle search and pursuit problems, where the targets are not stationary and sensor data are not entirely reliable [8]. The bird deterring problem can also be formulated as a 2D problem because all the grapes to be protected are located at ground level. The UAVs can be operated at a unique fixed altitude near ground level to avoid collision.

3 SYSTEM OVERVIEW

The following system hardware requirement is proposed based on extensive flight trials. Experiments were conducted in multiple vineyards located in south-east Australia [9]. The autonomous bird deterrent system being proposed consists of four sub-systems. They are the bird detection system; perceived predation risk generator system; flight control system; and ground control system. The organisation and communication between these sub-systems are illustrated in Figure 2.

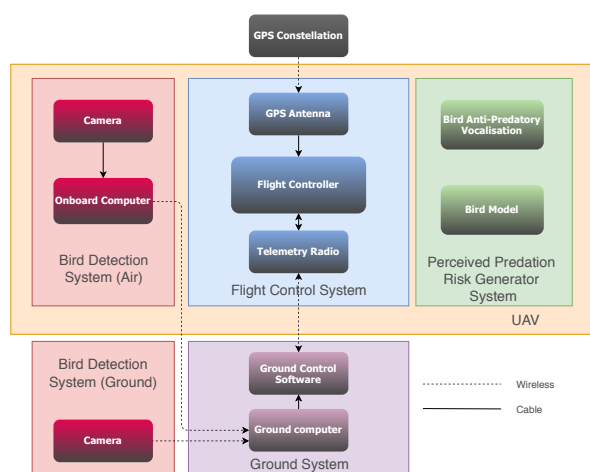


Figure 2: System diagram of the proposed UAV bird deterrent system.

3.1 Bird Detection System

The bird detection system consists of cameras on both the UAV platform and the ground. The camera on the UAV platform enables active tracking of the bird flock, whereas the ground camera can provide early warning of a bird attack. It is not necessary and inefficient energy-wise to have a UAV deployed all the time. The ground camera can be therefore used to decide whether a UAV should be deployed. The ground camera feeds the captured frames directly to the ground system computer for image processing. The frames captured by the air camera on the other hand are fed to an on-board computer for processing. The detection results are then transmitted to the ground computer using wireless communication.

3.2 Perceived Predation Risk Generator System

As mentioned in Section 2, the UAV should produce anti-predator vocalisation, as well as the source of the threat. We have chosen the combination of bird distress calls and a bird model to achieve this goal.

3.3 Flight Control System

The flight control system provides basic stabilisation, and more importantly, position control capabilities. The local position must be known for autonomous operations. GPS is one of the simplest methods, since the only additional hardware required is a GPS antenna. However, GPS lacks the accuracy other vision based methods have. High accuracy position control is always desirable for navigation in cluttered environment. Vineyards on the other hand are usually very open. Therefore, position control relying on GPS is sufficient for the problem.

3.4 Ground Control System

The ground control system is essentially a computer that processes videos from ground cameras for bird detection; runs path planning algorithm; communicates decisions with the flight control system; and monitors UAV status such as altitude, position and battery level through a ground control software.

3.5 UAV Platform

The appropriate UAV platform is determined to be a high endurance multirotor. Multirotors have many advantages over other UAV platforms. The ability to hover and to take-off/land vertically greatly reduce the burden on ground infrastructure. Multirotors are also very simple mechanically, which reduce the risk of failure. The only short-coming is the much lower endurance compared to fixed-wing UAV. However, a typical bird deterrent mission is less than 10min as we discovered in our trials.

4 DETERRING STRATEGY

A flow chart of the decision process is shown in Figure 3. When the system finishes initialising, the ground bird detection system is activated to detect pest birds. In the event of

a detection, the UAVs are launched. A trajectory is immediately planned by the ground control system for the UAVs to follow based on the current knowledge of bird location.

As the UAVs execute the mission, the ground control system constantly monitors the battery level of the UAVs. The UAVs are commanded to return home and land immediately if the battery level is lower than the safety threshold. Redundant UAVs are initialised if all other UAVs are insufficiently charged and birds have not left the vineyard. The on-board bird detection system simultaneously updates the bird location for the ground control system. All UAVs are sent home for landing once the birds are sufficiently far away from the vineyard.

5 MANUAL FLIGHT EXPERIMENT RESULTS

A series of manual flight trials were performed at multiple vineyards in south-east Australia to assess the effectiveness of the proposed system [9].

5.1 Experiment Set-up

In the manual flight experiment, all operations and decision making in Figure 3 were carried out manually by UAV operators. A multirotor UAV, as shown in Figure 1, was manually flown to deter pest birds. Birds were detected, and their response were recorded by observers with binoculars on the ground; perceived predation risk generator system was turned on manually at UAV launch; UAV position was controlled from the ground using a remote control transmitter; the relative distance between the bird and the UAV was estimated using the GPS data from the flight controller. The UAV po-

sition control was achieved by the flight controller Pixhawk running PX4, and the dedicated GPS module mRo U-Blox M8N GPS [10].

A piezoelectric tweeter was used to broadcast bird distress call. A piezoelectric tweeter was a better choice due to the louder volume at higher frequency compared to a magnet-driven speaker with similar size and weight. The source of the predation risk was a bird model mounted upside-down underneath the multirotor UAV, as shown in Figure 1.

5.2 Bird Response to UAV

On average, a 10min flight was sufficient to deter all pest birds off a 8 hectare vineyard. Some birds started fleeing 450m away from the UAV, all birds fled the initial location when the UAV was 50m away from them. The targeted bird flocks did not return at least 2 hours after UAV flight. We also determined the birds were only interested in feeding during early morning (6:00-10:00 AM) and late afternoon (4:00-7:00 PM) regardless of the presence of UAV.

The implication of these results was that it was not necessary for the UAV to chase after the birds directly. Instead, the UAV could be treated as a source of influence with a finite radius of effect. As a result, the UAV did not need to be a high speed and high manoeuvrability platform. Furthermore, the UAV did not need to operate throughout the entire day. The birds were only active 7 hours a day, and they did not return for at least 2 hours after a 10min UAV mission. This indicated that a high endurance UAV was not necessary, as there was plenty of time between the flights for battery recharging.

5.3 Bird Detection Results

While the UAV was operated manually, we took the opportunity to test the bird detection algorithm during the trials. The proposed algorithm utilised FAST (Features from Accelerated Segment Test) algorithm [11] to compensate global motion between consecutive frames. The pixel change between the two frames was then analysed with background subtraction using Gaussian mixture models [12] to isolate the actual birds from noises, such as moving leaves.

For bird detection in the air, the computer vision algorithm was implemented on the Raspberry Pi 3 Model B (1.2GHz CPU and 1GB of RAM, running Ubuntu MATE 16.04) [13] and the Raspberry Camera Module V2 [14]. For bird detection on the ground, a Panasonic DMC-FZ200 camera was used. The videos were processed on a Laptop running macOS 10.13.6, with a quad core 2.7GHz Intel Core i7 CPU and 16 GB of RAM. Both systems were able to process the incoming 720P 30FPS footage in real time. Figure 4 shows example frame from the processed footages. The algorithm detected all birds in the frame if the contrast between the birds and the background was high, as shown in Section 5.3; only 60% of the birds were detected in Section 5.3 since the contrast between the sky and the white cockatoos was very low. But the results were sufficient to determine the direction of the flock centroid.

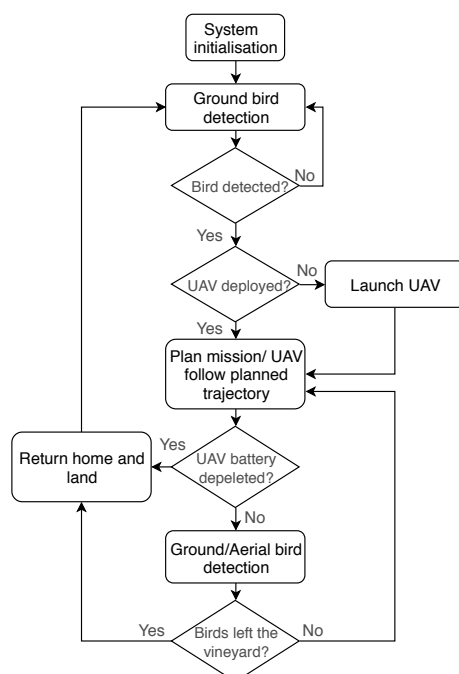
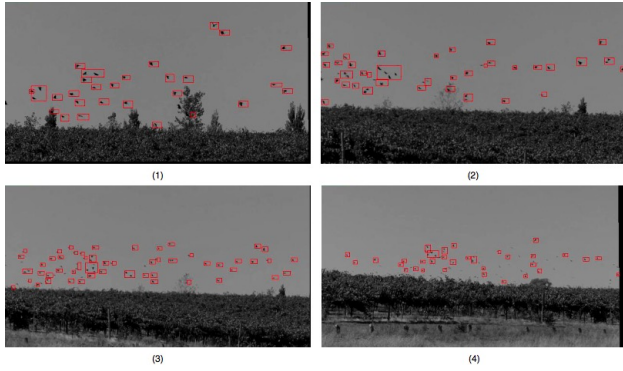
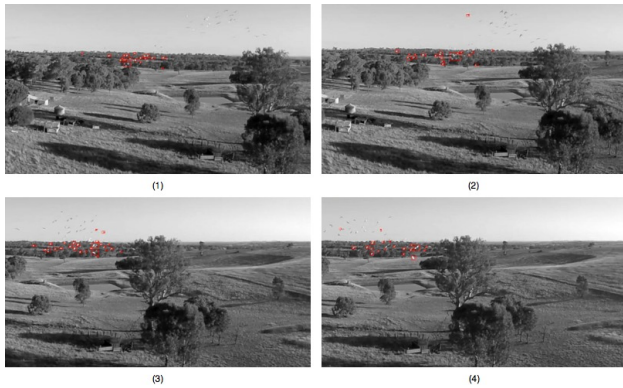


Figure 3: The decision process of the system.



(a) Detection result on ravens from ground camera



(b) Detection result on cockatoos from UAV camera

Figure 4: The proposed bird detection algorithm implemented. Detected birds are bounded by red boxes.

6 TOWARDS AUTONOMOUS SYSTEM

The manual flight experiment demonstrated the effectiveness of the UAV at deterring pest birds and the viability of the deterring strategy. A path planning algorithm is proposed in this section.

6.1 Environment Model

As discussed in Section 2, occupancy grid maps are useful when the system is not entirely confident about the target location, and the information is only relevant in 2D. The vineyard area to be protected can be represented by an 2D area that consists of cells of uniform size in the x dimension between x_{min} and x_{max} ; and in the y dimension between y_{min} and y_{max} . The spatial domain M of the occupancy map can thus be defined by Equation (1).

$$M = \left\{ \bar{c} \mid \begin{array}{l} \bar{c}_x \in [x_{min}, x_{max}] \\ \bar{c}_y \in [y_{min}, y_{max}] \end{array} \right\} \quad (1)$$

Each cell in the occupancy map is located by its coordinates \bar{c} . The occupancy map is then defined by a scalar number $k \in [0, 1]$ to each cell $\bar{c} \in M \subset \mathbb{R}^2$ at a certain time step $t \in \mathbb{R}$. The scalar number k is the probability indicator for the bird existence at each cell, $k = 1$ represents the system is 100% confident birds are located in that cell, and vice versa

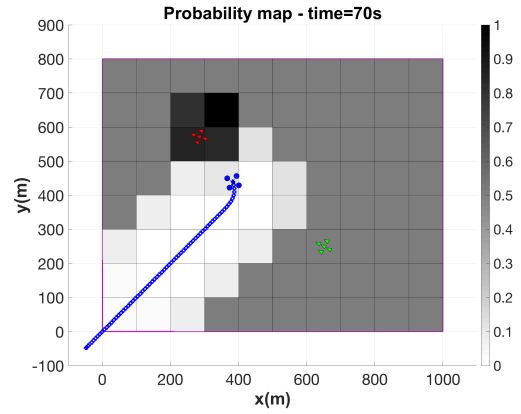


Figure 5: Probability map example.

for $k = 0$. The probability is updated at each time step by information from the bird detection system. This occupancy map is therefore a probability map of the target, an example of the map is shown in Figure 5. In the map, each bird flock is represented by 5 small triangles arranged in a cross (red and green in Figure 5). The UAV is represented by a small triangle surrounded by 4 circles (blue in Figure 5). The path taken by the UAV is indicated by a trail of markers corresponding to the UAV colour. A trail of low probability cells are visible along the UAV trajectory. The 4 cells adjacent to the red target have higher probability as it enters the UAV's sensor field-of-view.

Furthermore, the probability is time varying, it approaches a non-zero nominal value if no sensor information is available. It reflects the fact that the system's confidence about a cell gradually decreases. It also accounts for the possibility of birds returning to previously treated area. The probability approaches the nominal value k_{nom} according to Equation (2).

$$k(t + 1, \bar{c}) = \tau_{prob}k(t, \bar{c}) + (1 - \tau_{prob})k_{nom} \quad (2)$$

$\tau_{prob} \in [0, 1]$ is a time constant that dictates the rate at which k approaches k_{nom} .

6.2 Sensor Model

To model the camera, a circular sector of radius r_{sen} and angle θ_{sen} is placed at the centre of the simulated UAV, such that if no bird flock is inside the circular sector, all cells covered by the cone are assigned k_{low} . If any bird flock is inside the circular sector, cells within r_{unc} of the bird flock are assigned k_{high} as an estimation of the sensor uncertainty. This is illustrated in Figure 6. Ground sensor model can be estimated in a similar fashion.

6.3 UAV Model and Optimal Trajectory

The UAVs in the simulation have simple second-order dynamics based on the performance of the multirotor used in the manual experiments. The optimal trajectories for the UAVs are the trajectories that can minimise the probability of the entire map while also satisfying the constraints of the UAVs.

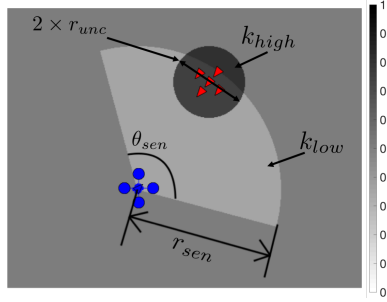


Figure 6: Sensor model illustration.

The algorithm first searches for the optimal cell the UAV is able to reach in the next n time steps. The set of cells C reachable by the UAV in n time steps are first selected according to the UAV's maximum velocity and turning rate. The probability states of these cells $k(t + n, \bar{c})$ are then predicted according to Equation (2). Multiple UAVs can achieve cooperation by taking other UAV's movement into $k(t + n, \bar{c})$ prediction. The problem then becomes an optimisation problem, described in Equation (3).

$$\underset{\bar{c} \in C}{\text{minimise}} \quad k(t + n, \bar{c}) + \alpha \cdot f_d(\bar{c}) + \beta \cdot f_h(\bar{c}) \quad (3)$$

The functions f_d and f_h compute the distance and the heading change required to reach the cell at \bar{c} . α and β are weights used to penalise distance and heading change to ensure smooth and efficient trajectories. This optimal cell is the next way-point for the UAV. The current strategy to find the optimal cell is by brute force. This will be improved in the future by employing a proper optimisation algorithm.

6.4 Bird Behaviour Model

The state of the bird x_{bird} is simplified to only position, velocity and heading, and it follows a simple second-order dynamics estimated from observed bird behaviour. We assign a second scalar number $i \in [0, 1]$ to each cell $\bar{c} \in M \subset \mathbb{R}^2$ at a certain time step $t \in \mathbb{R}$ to represent the birds' interest in visiting each cell. An example of the interest map is shown in Figure 7. The interest value gradually decreases to 0 at the UAV centre as indicated by the lighter cells in the figure.

To account for the likelihood of birds returning to treated area, i approaches a nominal value i_{nom} according to Equation (4) in a similar fashion as k . $\tau_{interest}$ is the time constant that determines the speed at which i approaches i_{nom} .

$$i(t + 1, \bar{c}) = \tau_{interest} i(t, \bar{c}) + (1 - \tau_{interest}) i_{nom} \quad (4)$$

The simulated birds move in the occupancy grid such that they maximise the interest in their surrounding cells. The optimisation problem is now defined by Equation (5).

$$\underset{\bar{c} \in C}{\text{maximise}} \quad i(t + n, \bar{c}) + \alpha \cdot f_d(\bar{c}) + \beta \cdot f_h(\bar{c}) \quad (5)$$

Similarly, the optimal cell is currently searched by brute force. An appropriate optimisation algorithm such as evolutionary algorithm will be investigated in the future.

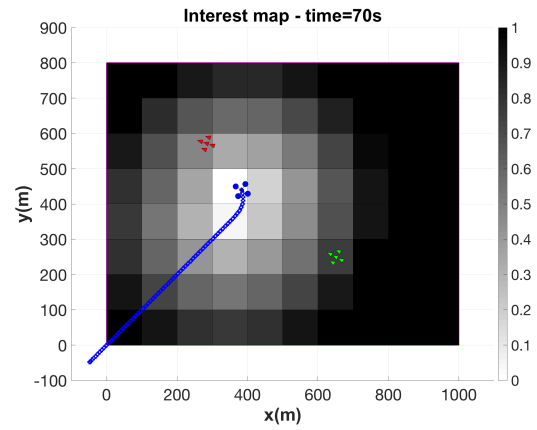


Figure 7: Interest map example.

7 SIMULATION RESULTS

Important simulation parameters are summarised in Table 1. Two flocks of birds (red and green) and two UAVs (blue and yellow) were initialised. No ground sensors were simulated, knowledge of the bird existence was assumed. According to observed bird behaviour, i is set to 0 within 50m of any UAVs, and i increases linearly to 1 at 450m away from any UAVs as a conservative estimate.

Snapshots of the simulation are included in Figure 8. In Figure 8a, all cells were initialised with $k = 0.5$. At $t=30s$, in Figure 8b, both UAVs were following a straight line as no birds were detected. The yellow UAV detected the green flock, hence the probability increased in the region. At $t=60s$, shown in Figure 8c, the blue UAV joined the green UAV to chase the green flock. In Figure 8d, both flocks were successfully deterred as they left the environment. The simulation demonstrated that two flocks of birds on an 8 hectare area can be effectively deterred using the proposed algorithm.

8 CONCLUSION AND FUTURE RESEARCH

Bird damage is a very challenging global problem. The solution proposed in this research incorporates bird psychology and autonomous UAVs to overcome the limitation in other methods. A bird deterring strategy and a bird chas-

Table 1: Simulation parameters

Parameter	Value	Parameter	Value
Cell shape	square	Cell size	10×10 m
x_{min}	0 m	$\tau_{interest}$	0.99
x_{max}	1000 m	τ_{prob}	0.99939
y_{min}	0 m	k_{nom}	1
y_{max}	800 m	k_{low}	0.2
UAV max. velocity	10 m/s	k_{high}	0.8
UAV max. yaw rate	45 deg/s	θ_{sen}	120°
Bird max. velocity	8 m/s	r_{unc}	100 m
Bird max. yaw rate	20 deg/s	r_{sen}	200 m

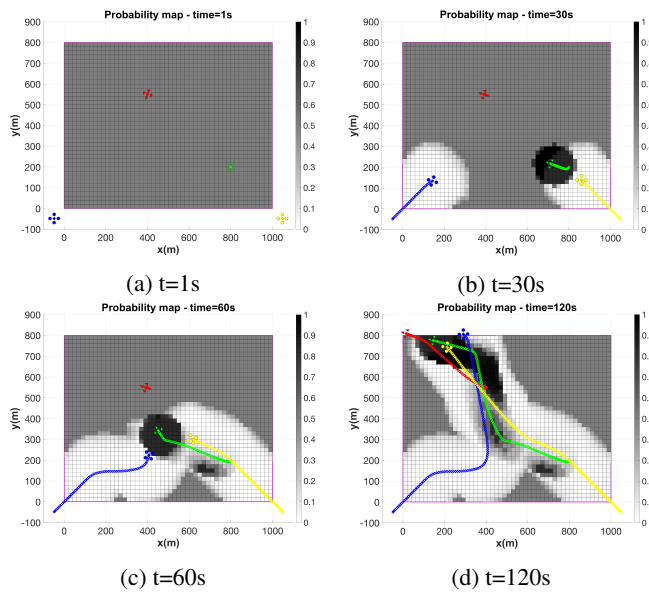


Figure 8: Simulation results

ing algorithm were developed to enable autonomous operation of the proposed system. Simulation results indicated the system had potential in protecting a large vineyard with multiple UAVs. Future research is needed in coordinating multiple UAVs to execute the mission more efficiently. The cost function needs to be adjusted to avoid multiple UAVs chasing after the same flock. Despite the openness of agriculture properties, no-fly region may exist due to high trees or power poles. Future research should modify the cost function to take no-fly region into consideration. Current research is directed towards applying this algorithm on hardware.

ACKNOWLEDGEMENTS

We would like to thank Dr. Andrea Griffin from the University of Newcastle, Darren Fahey from New South Wales Department of Primary Agriculture and Dr. Andrew Lucas from Agent Oriented Software for their support in our manual flight experiment.

REFERENCES

- [1] John Tracey, M Bomford, Quentin Hart, Glen Saunders, and Ron Sinclair. *Managing bird damage to fruit and other horticultural crops*. Bureau of Rural Science, Canberra, 2007.
- [2] J. L. Elser, A. Anderson, C. A. Lindell, N. Dalsted, A. Bernasek, and S. A. Shwiff. Economic impacts of bird damage and management in U.S. sweet cherry production. *Crop Protection*, 83:9–14, 2016.
- [3] Michael R. Conover. *Resolving Human-Wildlife Conflicts*. CRC Press, Boca Raton, FL., 2001.
- [4] Sara M. Kross, Jason M. Tylanakis, and Ximena J. Nelson. Effects of Introducing Threatened Falcons into

Vineyards on Abundance of Passeriformes and Bird Damage to Grapes. *Conservation Biology*, 26(1):142–149, 2012.

- [5] Brian A. Grimm, Brooke A. Lahneman, Peter B. Cathcart, Robert C. Elgin, Greg L. Meshnik, and John P. Parmigiani. Autonomous Unmanned Aerial Vehicle System for Controlling Pest Bird Population in Vineyards. In *Volume 4: Dynamics, Control and Uncertainty, Parts A and B*, page 499. ASME, nov 2012.
- [6] Michael R. Conover and James J. Perito. Response of Starlings to Distress Calls and Predator Models Holding Conspecific Prey. *Zeitschrift für Tierpsychologie*, 57(2):163–172, 1981.
- [7] Andrea S. Griffin, Hayley M. Boyce, and Geoff R. MacFarlane. Social learning about places: observers may need to detect both social alarm and its cause to learn. *Animal Behaviour*, 79(2):459–465, 2010.
- [8] Christopher W Lum, Rolf T Rysdyk, and Anawat Pongpunwattana. Occupancy based map searching using heterogeneous teams of autonomous vehicles. *AIAA Guidance, Navigation, and Control Conference and Exhibit*, (August):1–15, 2006.
- [9] Zihao Wang, Andrea S. Griffin, Andrew Lucas, and KC Wong. Psychological warfare in vineyard: using drones and bird psychology to control bird damage to wine grape. *Unpublished manuscript*, 2018.
- [10] MRobotics. mRo Pixhawk 2.4.6 Cool Kit (Limited edition), url: <https://store.mrobotics.io/product-p/mro-pixhawk1-fullkit-mr.htm>, 2016.
- [11] E. Rosten, R. Porter, and T. Drummond. Faster and Better: A Machine Learning Approach to Corner Detection. *IEEE Transactions on Pattern Analysis and Machine Intelligence*, 32(1):105–119, jan 2010.
- [12] C. Stauffer and W.E.L. Grimson. Adaptive background mixture models for real-time tracking. In *Proceedings. 1999 IEEE Computer Society Conference on Computer Vision and Pattern Recognition (Cat. No PR00149)*, pages 246–252. IEEE Comput. Soc, 1999.
- [13] Eben Upton. Raspberry Pi 3 Model B, url:<https://www.raspberrypi.org/blog/raspberrypi-3-model-bplus-sale-now-35/>, 2018.
- [14] Raspberry Pi Foundation. Camera Module, url:<https://www.raspberrypi.org/documentation/hardware/camera/README.md>, 2016.